Time-Resolved and Static Resonance Raman Spectroscopy of Horseradish Peroxidase Intermediates†

W. Anthony Oertling and Gerald T. Babcock*

Department of Chemistry, Michigan State University, East Lansing, Michigan 48824-1322

Received November 5, 1987; Revised Manuscript Received December 28, 1987

ABSTRACT: By using pulsed and continuous wave laser irradiation in the 350–450-nm region, we have characterized Raman scattering from horseradish peroxidase (HRP) compounds I and II and from iron porphyrin π-cation radical model compounds. For compound II we support the suggestion [Terner, J., Sitter, A. J., & Reczek, C. M. (1985) *Biochim. Biophys. Acta 828*, 73–80; Proniewicz, L. M., Bajdor, K., & Nakamoto, K. (1986) *J. Phys. Chem. 90*, 1760–1766] that resonance enhancement of the Fe^{IV}=O vibration proceeds by way of a charge-transfer state. Our excitation profile data locate this state at ~400 nm. Compound I was prepared at neutral pH by rapid mixing of the resting enzyme with hydrogen peroxide. Each sample aliquot was excited by a single, 10-ns laser pulse to generate the Raman spectrum; optical spectroscopy following the Raman measurement confirmed that HRP-I was the principal product during the time scale of the measurement. The Raman spectrum of this species, however, is not characteristic of that which we observe from metalloporphyrin π-cation radicals [Oertling, W. A., Salehi, A., Chung, Y., Leroi, G. E., Chang, C. K., & Babcock, G. T. (1987) *J. Phys. Chem. 91*, 5887–5898], including the iron porphyrin cation radicals reported here. Instead, the spectrum recorded for HRP-I at neutral pH is suggestive of an oxoferryl heme with the same geometric and electronic structure as that of HRP-II at high pH. The similarity between the two species extends to the Fe=O stretching vibration, which we observe in the transient species at a frequency (791 cm^{-1}) and with an intensity typical of the high pH, non-hydrogen-bonded form of HRP-II. We consider two interpretations of these data: (a) extensive delocalization of the porphyrin π-cation radical of HRP-I onto the axial ligands and (b) rapid and efficient photoinduced electron transfer to the porphyrin radical of HRP-I to produce a new species, HRP-I*, from which Raman scattering is observed.

Horseradish peroxidase (HRP) uses hydrogen peroxide to catalyze the oxidation of indoleacetic acid in plant roots. The prosthetic group of the resting enzyme consists of a ferric protoporphyrin IX ligated on the proximal side of the heme plane by histidine nitrogen. Distinct transient states are formed during catalysis. In the first intermediate, compound I (HRP-I), the heme most likely retains the histidine imidazole (Im) ligand and undergoes two-electron oxidation, forming an oxoferryl[1] protoporphyrin IX π-cation radical, $O{=}Fe^{IV}(Im)PP^{\bullet+}$. The second intermediate, compound II (HRP-II), is formed via the oxidation of the substrate, which leaves the low-spin ($S = 1$) oxoferrylimidazole linkage intact but reduces the porphyrin macrocycle to the neutral state (Dunford, 1982; Frew & Jones, 1984). The intermediates of the HRP reaction are likely to be similar to structures that occur during catalysis by other peroxidases and also by catalases, oxygenases, and oxidases (Naqui & Chance, 1986).

The oxoferryl structure of HRP-I and HRP-II is well characterized by a variety of physical techniques (Frew & Jones, 1984). In particular, recent evidence from extended X-ray absorption fine structure (EXAFS) spectroscopy indicates structures for HRP-I and HRP-II with relatively short (1.65 Å) Fe=O bond lengths and contracted (1.99 Å) heme center to pyrrole nitrogen distances (Penner-Hahn et al., 1986). Recent resonance Raman (RR) measurements of the Fe=O stretching frequency, ν(Fe=O), of HRP-II (Terner et al., 1985; Hashimoto et al., 1984) and model oxoferryl porphyrins (Proniewicz et al., 1986; Chappacher et al., 1986; Kean et al., 1987; Hashimoto et al., 1987) confirm the double-bonded character and short bond length of the oxoferryl structure. Furthermore, the frequencies of the porphyrin core vibrational modes are consistent with the 1.99-Å core size for HRP-II (Sitter et al., 1985a) and for the synthetic oxoferryl complexes (R. T. Kean, W. A. Oertling, and G. T. Babcock, unpublished results). In the synthetic oxoferryl species, the resonance enhancement of the Fe=O stretching vibration has been suggested to result from the occurrence of a charge-transfer transition near the heme Soret band (Terner et al., 1985; Proniewicz et al., 1986). We report here HRP-II excitation profile measurements that support this hypothesis.

Although RR techniques have been extensively applied to HRP-II and its models, RR studies of the first intermediate, HRP-I, are complicated by its reactivity and photolability (Stillman et al., 1975). Past studies (Van Wart & Zimmer, 1985) indicated that cryogenic techniques are insufficient to stabilize HRP-I to laser irradiation in the Soret region (350–450 nm). Because of this we adopted an alternative approach in which pulsed, near-UV RR excitation of flowing samples of HRP-I generated by rapid mixing is used (Oertling & Babcock, 1985). The key to this method is that a fresh sample of HRP-I is used for each laser pulse in accumulating the spectrum. The high-frequency (1200–1700 cm^{-1}) spectrum of HRP-I we obtained with this technique has been recently confirmed by Ogura and Kitagawa (1987) with continuous wave (CW) excitation. At the time of our initial report of the HRP-I spectrum, RR scattering by metalloporphyrin π-cation

† This work was supported by NIH Grant GM 25480.

[1] Ferryl is used to represent iron(IV). IUPAC recommends ferrio in the context used in this paper.

0006-2960/88/0427-3331$01.50/0

radicals had not been characterized. Since then, however, we have carried out an extensive RR study of metalloporphyrin π-cation radicals ($MP^{\bullet+}$) (Salehi et al., 1986, 1987; Oertling et al., 1987 a,b, 1988). Using these $MP^{\bullet+}$ results, additional model compound data, and further characterization of RR scattering from HRP-II, we have reanalyzed the high-frequency RR spectrum obtained for HRP-I at pH 7. We find no vibrational frequencies characteristic of a metalloporphyrin π-cation radical ($MP^{\bullet+}$). We have also obtained the low-frequency RR spectrum for this species and have located a band that we assign to the Fe=O stretching vibration. The frequency of this mode is distinct from that of HRP-II at neutral pH. In view of the evidence in favor of the $P^{\bullet+}$ formulation for HRP-I from various spectroscopies (Dolphin et al., 1971; Hewson & Hager, 1979; Dunford, 1982; Frew & Jones, 1984), we consider possible explanations for the RR results.

Materials and Methods

Horseradish peroxidase was purchased from Sigma (Type VI) and used without further purification. Sodium phosphate and sodium carbonate buffers (50 mM) were used at pH 7 and 10.8, respectively, for all enzyme and hydrogen peroxide solutions. $H_2{}^{16}O_2$ (30%) was purchased from Mallinckrodt. $H_2{}^{18}O_2$ was made from $^{18}O_2$ (98%, Cambridge Isotope Laboratories) by using glucose oxidase according to the procedure of Asada and Badger (1984). HRP and peroxide solutions were quantified photometrically by using extinction coefficients at 403 (Schonbaum & Lo, 1972) and 240 nm (Worthington, 1972) of 103 and 43.6 M^{-1} cm^{-1}, respectively.

Flowing HRP-I samples (pH 7) for RR measurements were prepared by rapid mixing of equal volumes of cooled solutions of 0.1 mM HRP and 1 mM hydrogen peroxide. These were loaded in 10.0-mL syringes and driven through two eight-jet tangential mixers in series with a Sage 355 syringe pump (Oertling & Babcock, 1985). After mixing, the HRP-I sample passed through a 0.5-mm i.d. capillary. Raman scattering from HRP-I was measured both with pulsed excitation at 390 and 420 nm and with CW excitation at 406.7 nm. HRP-I samples prepared from recycled solutions had a much longer lifetime owing to the removal of potential substrates present in the preparations (Chance, 1949). RR spectra of HRP-I were obtained by using 0.22–0.85 mL/min flow rates which produced dead times of 9.3–2.4 s between mixing and laser excitation, respectively. These flow rates ensured that 2.3–4.7 scattering volumes, respectively, passed through the capillary between laser pulses. Thus, each pulse was incident on a fresh sample aliquot.

The formation of HRP-I was confirmed for each rapid mixing experiment by visual detection of the flowing green solution in the capillary at the onset of the RR measurement. Immediately after laser irradiation, a sample aliquot was collected for a UV–visible absorption measurement. For the recycled samples these spectra were essentially that of HRP-I. For the less stable fresh samples these spectra reflected a mixture of HRP-I and HRP II. The total time from mixing to the absorption spectrum was typically 3–5 min. The formation of HRP-I prior to the RR measurement was further confirmed by an independent optical absorption experiment in which the rapid mixer with a section of rectangular tubing (0.3-mm path, Vitrodynamics) was used in place of the capillary. Under mixing conditions that reproduced those in the Raman work, the characteristic Soret absorption of HRP-I was obtained.

HRP-II samples were prepared in a cooled cylindrical quartz cell that was spun during RR measurements. Addition of

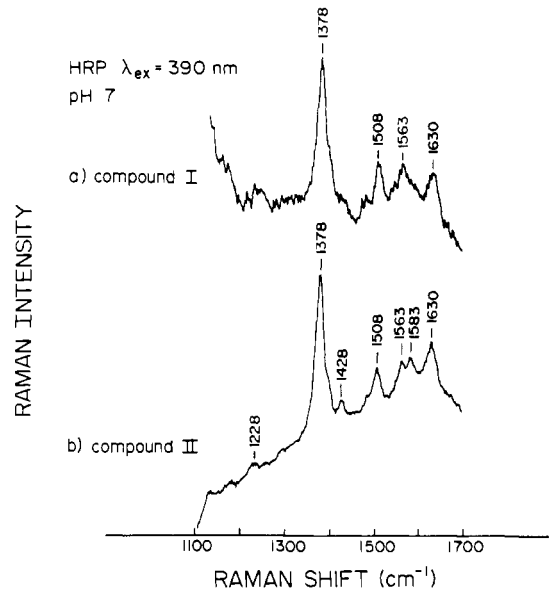

FIGURE 1: High-frequency RR spectra of HRP samples at 2–10 °C, 1 mJ/pulse. Sample conditions and total accumulation times: (a) flowing in the capillary of the rapid mixer at 0.65–0.85 mL/min, 40 min; (b) spinning cell, 22 min.

stoichiometric amounts of *p*-cresol (Aldrich) and 1.5× stoichiometric quantities of hydrogen peroxide to solutions of native HRP at pH 7 resulted in the formation of HRP-II. RR spectra of these samples were collected with optical multichannel analyzer detection for 2.5 min, after which time absorption spectra were monitored and the experiment was repeated with a fresh sample. HRP-II samples at pH 10.8 were prepared by adding 1.5 equiv of peroxide to solutions of the native enzyme. RR spectra of these more stable solutions were collected for 10 min, and absorption spectra, which confirmed sample integrity, were monitored before and after laser irradiation.

Oxidation of ferric complexes of octaethyloporphyrin (FeOEP) and protoporphyrin IX dimethyl ester (FePPIX) to the corresponding π-cation radical species was performed by A. Salehi as described elsewhere (Salehi et al., 1987). CH_2Cl_2, freshly distilled from CaH_2, was used as the solvent. Sample integrity was confirmed by optical absorption before and after RR measurements.

Laser pulses (10-ns duration, 10 Hz) from 390 to 435 nm were provided by a DCR-1A-based Quanta Ray system by using three laser dyes (Exciton): LD390 (in methanol), DPS (in dimethylformamide), and Stilbene 420 (in methanol). CW emission at 351.1 and 363.8 nm came from a Coherent Innova 90-5 argon ion laser. Raman scattering from these sources was measured with a Spex/EG&G PAR diode array spectrometer as described (Oertling & Babcock, 1985). Instrumentation used to measure Raman scattering from the 406.7-nm krypton ion laser (Spectra Physics 164-11) emission was based on a Spex 1401 double-monochromator (Oertling et al., 1987b). UV–visible absorption spectra were measured with a Perkin-Elmer Lambda 5.

Results

High-Frequency RR Scattering from HRP Intermediates. Figure 1 shows the RR spectra of HRP-I and HRP-II. The similarity of the 390-nm RR spectra of these two intermediates is surprising considering the significant differences we observe in the vibrational frequencies and RR intensities of metalloporphyrin π-cation radicals ($MP^{\bullet+}$) and their neutral metalloporphyrin (MP) parent compounds (Salehi et al., 1986;

Table I: Vibrational Assignments (1450–1700 cm^{-1}) for Ferric Porphyrins and Their π-Cation Radicals

	ClFeOEP	ClFeOEP$^{\bullet+}$	ClFePPIX	ClFePPIX$^{\bullet+}$
$\nu_3(C_aC_m)$	1494	1486	1493	1490
$\nu_{11}(C_bC_b)$	1559	~1577	1553	~1570
$\nu_2(C_bC_b)$	1581	1602	1572	~1593
$\nu_{37}(C_aC_m)$			1590	~1585
$\nu_{10}(C_aC_m)$	1629	1625	1630	1628

Oertling et al., 1987b). This strong similarity was obscured in our previous analysis of the high-frequency RR spectrum of HRP-I (Oertling & Babcock, 1985) because we compared it to RR spectra of HRP-II produced with excitation at 514.5 or 457.9 nm from early work (Felton et al., 1976; Rakhit et al., 1976). Our spectra of HRP-II with excitation from 390 to 435 nm match more recent work with 406.7-nm excitation (Terner & Reed, 1984; Hashimoto et al., 1984), and a reanalysis of our high-frequency RR spectrum of HRP-I is necessary. In accord with previous work (Abe et al., 1978; Terner & Reed, 1984), we assign the bands at 1378, 1508, 1563, and 1630 cm^{-1} from the RR spectra in Figure 1 to ν_4, ν_3, ν_{11} overlapped with ν_{38}, and ν(C=C), respectively, for both HRP-I and HRP-II. The resonance enhancement of ν_{10} at this excitation wavelength is negligible (see below). Thus, the spectra differ only in the relative intensity of the ν_2 mode, which appears at 1583 cm^{-1} in the spectrum of HRP-II and is all but absent in the spectrum of HRP-I.

High-Frequency RR Scattering from Iron Porphyrin π-Cation Radicals. Figure 2 depicts the RR spectra of a ferric octaethylporphyrin π-cation radical, $Cl^-Fe^{III}OEP^{\bullet+}SbCl_6^-$, and its parent compound, $Cl^-Fe^{III}OEP$. Also shown are the spectra of the analogous protoheme species (Figure 2c,d). Using RR measurements, we have recently demonstrated that the OEP compounds exhibit a five-coordinate, high-spin ($S = {}^5/_2$) configuration for the heme iron in solution (Salehi et al., 1987); the protoheme spectra are consistent with the same spin and coordination state assignment for these species. Table I collects the vibrational assignments for these complexes. For the ferric OEP complexes, these assignments have been confirmed by deuterium substitution at the methine positions of the porphyrin (Oertling et al., 1988). The decrease in frequency for modes with significant C_bC_b character for the protoheme species relative to the OEP species is expected on the basis of the different pattern of peripheral substitution (Callahan & Babcock, 1981). The protoheme RR spectra are more complex owing to the E_u modes, ν_{38} and ν_{37}, which occur at 1530 and ~1553 cm^{-1}, respectively, in the neutral form (Figure 2c) (Choi et al., 1982). The position of ν_{38} in the cation radical is difficult to determine from our RR spectra excited at 351.1 (figure 2d) and 363.8 nm (not shown) but presumably can be measured with IR spectroscopy (Oertling et al., 1987b). We interpret the broad feature extending from 1570 to 1600 cm^{-1} in the $Fe^{III}PPIX^{\bullet+}$ spectrum to be composed of three overlapping bands: ν_{11} (C_bC_b) occurring at ~1570 cm^{-1}, ν_2 (C_bC_b) at ~1593 cm^{-1}, and ν_{37} (C_aC_m) at ~1585 cm^{-1}. The ~20-cm^{-1} increase in the modes (ν_{11}, ν_2) that are predominantly composed of C_bC_b stretches is expected upon oxidation of ferric porphyrin π-cation radicals (Salehi et al., 1987). These frequency increases are partially obscured in the spectrum in Figure 2d by the frequency decrease of ν_{37} (C_aC_m) in the cation (~1585 cm^{-1}) relative to that in the neutral (1590 cm^{-1}). These spectra demonstrate that the changes in the vibrational frequencies that accompany ring oxidation of these ferric compounds are consistent with those we have observed with other $MOEP^{\bullet+}$ species. In general, we find that stretching modes with predominantly C_aN character

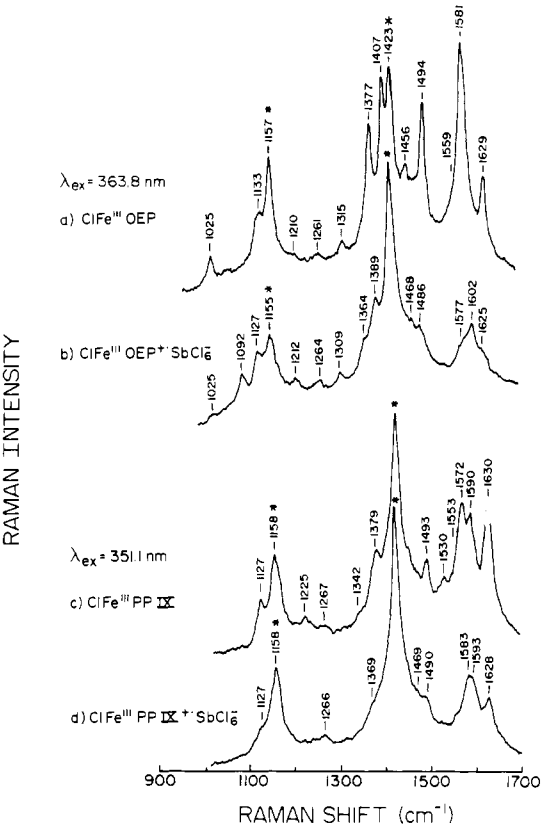

FIGURE 2: RR spectra of model compounds in CH_2Cl_2. Conditions: 25–30 mW incident on the sample in a spinning cell at 25 °C. Accumulation times: (a) 9.6 min; (b) 8.6 min; (c) 7.2 min; (d) 7.2 min. An asterisk indicates solvent band.

(ν_4) or C_aC_m character (ν_3 and ν_{10}) decrease in frequency, while those with C_bC_b character (ν_{11} and ν_2) increase in frequency when the porphyrin ring is oxidized (see Table I). We see these frequency shifts regardless of whether the electron is extracted from the $a_{1u}(\pi)$ or $a_{2u}(\pi)$ molecular orbital (Oertling et al., 1987b).

Low-Frequency RR Scattering from HRP Intermediates. Figure 3 shows low-frequency RR scattering from pulsed, 390-nm excitation of HRP, HRP-I, and HRP-II. The spectrum of the native enzyme, Figure 3a, is similar to that measured with 406.7-nm excitation (Terner et al., 1985); however, there are some differences in relative intensities produced by the different excitation frequencies. Spectra of HRP-I at pH 7, prepared with both $H_2{}^{16}O_2$ and $H_2{}^{18}O_2$, appear in Figure 3b. The feature at 791 cm^{-1} in the spectrum of the ^{16}O sample is replaced by a band at 754 cm^{-1} in the ^{18}O sample. The 35-cm^{-1} decrease in this mode upon substitution of ^{18}O for ^{16}O is expected for a Fe=O harmonic oscillator and, accordingly, this band is assigned to ν(Fe=O), the symmetric stretch of the oxoferryl of HRP-I.

Parts c and d of Figure 3 show spectra of HRP-II at pH 7 and 10.8, respectively. As shown by recent work (Terner et al., 1985; Hashimoto et al., 1986), at pH 7 the oxoferryl stretch of HRP-II appears as a weak feature at 774–779 cm^{-1} upon substitution of ^{18}O for ^{16}O. Our RR spectrum (Figure 3c) obtained at λ_{ex} = 390 nm of the second intermediate at pH 7 is consistent with these findings. On the other hand, for HRP-II at pH 10.8, RR excitation at 390 nm results in strong enchancement of ν(Fe=O) as shown in Figure 3d. Our results at pH 10.8 match those of Hashimoto et al. (1986) and Sitter et al. (1985b). We find ν(Fe=O) at 787 cm^{-1} for HRP-II at high pH, shifting to 753 cm^{-1} upon ^{18}O substitution. Thus, ν(Fe=O) measured for HRP-I at pH 7 appears to be almost

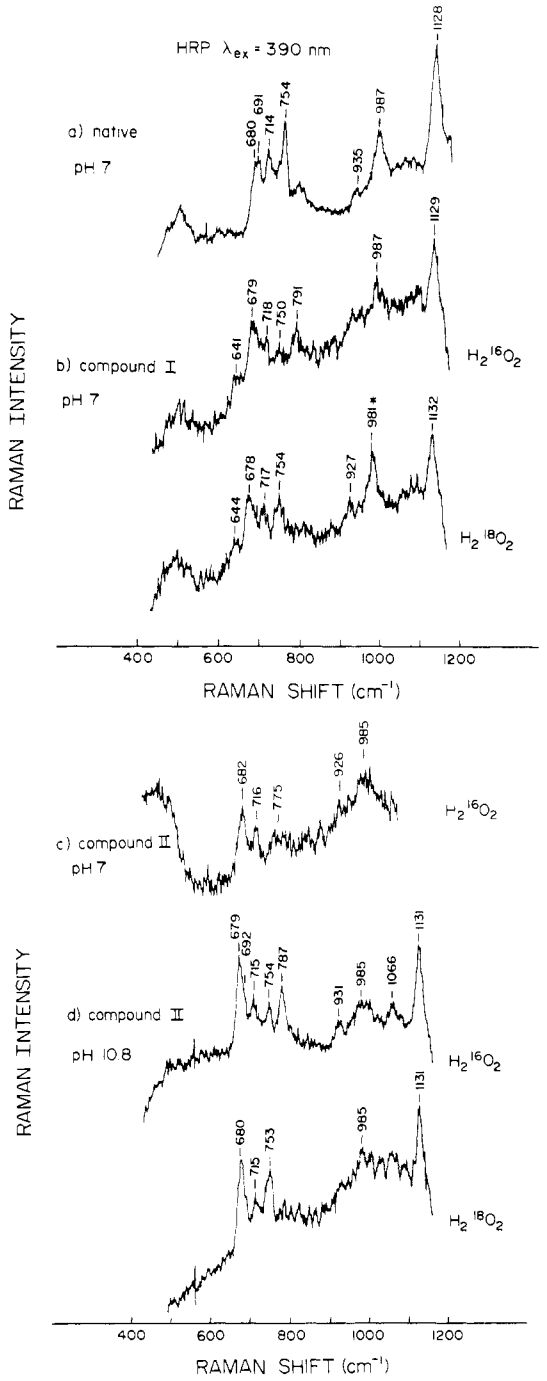

FIGURE 3: Low-frequency RR spectra of HRP samples obtained under 390-nm excitation. Total accumulation times: (a) 85 min; (b) ^{16}O sample 144 min, ^{18}O sample 78 min; (c) 52 min; (d) ^{16}O sample 48 min, ^{18}O sample 48 min. The feature at 981 cm^{-1} in (b) is due to sulfate ion in the $H_2{}^{18}O_2$ preparation.

identical with that of HRP-II at pH 10.8 in terms of both frequency and relative intensity. By analogy to earlier work this suggests that the oxo ligand of HRP-I is not hydrogen-bonded at pH 7 as is the case for HRP-II (Sitter et al., 1985b; Hashimoto et al., 1986).

In view of the model compound spectra presented in Figure 2 and elsewhere (Salehi et al., 1986, 1987; Oertling et al., 1987 a,b, 1988), the similarity of the high-frequency spectra of the enzyme transients presented in Figure 1 implies that the HRP-I spectrum we obtain is not characteristic of an oxoferryl porphyrin π-cation radical. The spectrum of this transient enzyme species is also distinct from that of HRP-II at neutral pH. They differ in the relative intensities of the high-frequency spectrum. In the low-frequency region, both the frequency

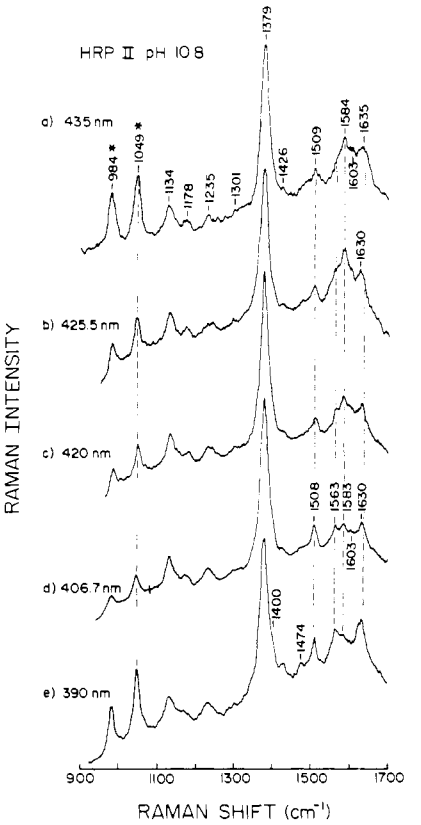

FIGURE 4: High-frequency RR scattering from HRP-II, pH 10.8. Accumulation time for each spectrum was 10 min with 1 mJ/pulse. Excitation wavelengths were as indicated. The 1049-cm^{-1} peak is from 0.2 M NO_3^- used as an internal standard to measure relative intensities. The 984-cm^{-1} feature is from SO_4^-.

and relative intensity of the ν(Fe=O) mode differ for these two species, and an additional feature occurs at 641–644 cm^{-1} in the HRP-I spectrum that is not apparent in the HRP-II spectrum. Moreover, optical absorption spectra recorded after each HRP-I Raman measurement indicated that HRP-I was the principal species present (see Materials and Methods). Reduction of HRP-I to HRP-II, either by photoreduction or by reduction by impurities acting as substrates, would be irreversible. Thus, HRP-II contaminants in the HRP-I sample are not the cause of the similar RR spectra of the two intermediates (Figure 1).

Soret Excitation Profiles for HRP Intermediates. The similarity between our RR results for HRP-I at pH 7 and HRP-II at pH 10.8 prompted us to examine the spectrum of both the second intermediate at high pH and the first intermediate at neutral pH as a function of excitation frequency. Figure 4 shows the spectrum of HRP-II at pH 10.8 at five excitation frequencies between 435 and 390 nm. Because the differences in the high-frequency spectra of HRP-I and HRP-II, both at pH 7 (Figure 1), are limited to the relative intensities of the features at 1563 and 1584 cm^{-1}, the behavior of these bands is of principal interest. With 435-nm excitation of HRP-II (Figure 4a) high-frequency bands appear at 1509 (ν_3), 1584 (ν_2), 1603 (ν_{37}), and 1635 cm^{-1} (ν_{10}). Figure 4b shows that the ν_{10} intensity falls off quickly as λ_{ex} moves to the blue and that with 425.5-nm excitation the ν(C=C) mode at 1630 cm^{-1} begins to dominate this region. Also, at this excitation wavelength, a shoulder is apparent at 1563 cm^{-1}. In parts c–e of Figure 4 this feature becomes more obvious as the excitation wavelength is varied toward higher energy, while the intensity of ν_2 (1584 cm^{-1}) decreases. Finally, with 390-nm excitation (Figure 4e), the feature at 1563 cm^{-1}

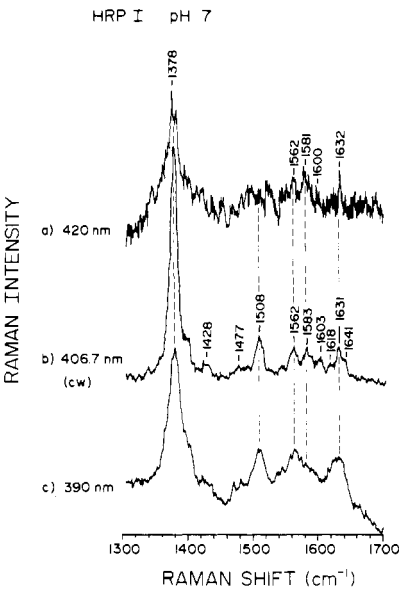

FIGURE 5: High-frequency RR scattering from HRP-I, pH 7: (a) 1.9 mJ/pulse, 4-min accumulation time; (b) 15 mW, CW excitation, 0.5 s/cm^{-1}, sample flow rate 0.22 mL/min (similar results were obtained flowing at 0.7 mL/min); (c) 1 mJ/pulse, 40-min accumulation time.

dominates this region of the spectrum, and the 1584-cm^{-1} mode now appears as a shoulder. Figure 5 shows RR scattering from our flowing HRP-I sample at pH 7 at three excitation frequencies in the Soret region. Although the spectrum excited at 420 nm (Figure 5a) is very weak owing to the poor resonance condition and short accumulation time, the dominant features can be recognized. The intensity of ν_2 (1581 cm^{-1}) is greater relative to the intensity of the band at 1562 cm^{-1} at this excitation wavelength. The spectrum in Figure 5b was obtained under CW excitation at 406.7 nm. Figure 5c juxtaposes the scattering excited at 390 nm with the other HRP-I spectra. Comparison of Figure 4c–e with Figure 5a–c suggests that the RR excitation profiles of the vibrational modes of the scattering species in the HRP-II, pH 10.8, and HRP-I, pH 7, samples are similar. In both cases the ν_2 mode at ~1583 cm^{-1} dominates the region from 1550 to 1600 cm^{-1} with 420-nm excitation, while a feature at ~1563 cm^{-1} dominates with 390-nm excitation. The intensities of these features are roughly equal with λ_{ex} = 406.7 nm.

The large relative intensity of the oxoferryl stretch in the RR spectra excited at 406.7 nm of HRP-II, oxoferryl myoglobin (Sitter et al., 1985a), and model compounds led to the suggestion of a charge-transfer (CT) electronic transition along the oxoferryl axis (Terner et al., 1985; Proniewicz et al., 1986). Figure 6 shows RR spectra of HRP-II (pH 10.8) obtained with seven excitation wavelengths from 432 to 390 nm. The ν(Fe=O) mode is obvious only in spectra produced with excitation to the blue of 410 nm, significantly higher in energy than the Soret absorption maximum at 419 nm. An excitation profile (a plot of relative Raman intensity vs excitation frequency, λ_{ex}) of the ν(Fe=O) = 787 cm^{-1} vibration is shown in Figure 7. Along with this, the excitation profiles of the porphyrin core vibrations, ν_7 = 680 cm^{-1} and ν_4 = 1379 cm^{-1}, are also displayed. The excitation profiles for the latter two HRP-II modes agree well with the excitation profiles for the corresponding ν_7 and ν_4 modes, respectively, of deoxymyoglobin observed by Bangcharoenpaurpong et al. (1984) and are consistent with π–π^* enhancement. However, the excitation profile of the axial Fe=O vibration in HRP-II contrasts markedly with that of the out-of-plane Fe—N(histidine) mode in deoxymyoglobin. The excitation profile of the latter vibration matches the Soret absorption of deoxymyoglobin, which was interpreted to indicate π–π^*, rather than charge transfer, enhancement of the Fe–N(histidine) mode. The excitation profile of the Fe=O vibration of HRP-II displayed in Figure 7, however, has a maximum around 400 nm, well to the blue of the Soret absorption maximum. This is consistent with the occurrence of a CT transition on the high-energy side of the Soret transition of HRP-II and with enhancement of the Fe=O stretching mode through this electronic transition.

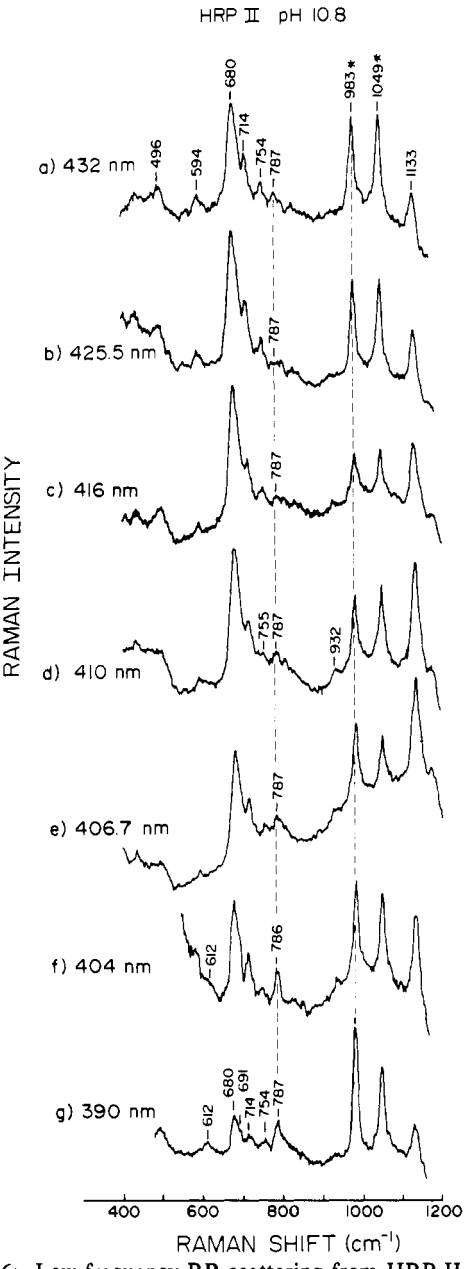

FIGURE 6: Low-frequency RR scattering from HRP-II, pH 10.8. Accumulation time was 10 min for (a–d) and 20 min for (e–g) with 1 mJ pulses. The 983-cm^{-1} peak is from 0.2 M $SO_4^{=}$, which was used as an internal intensity standard. The 1049-cm^{-1} feature is from NO_3^-.

DISCUSSION

If we consider that HRP-I contains a protoheme cation radical, then we can use our structural correlations for MOEP$^{\bullet+}$ complexes (Oertling et al., 1987b) and the data in Figure 2 to predict its high-frequency Raman modes. Assuming a core size of 1.99 Å (Penner-Hahn et al., 1986), we expect ν_3, ν_{11}, and ν_2 to occur at approximately 1501, 1593, and 1607 cm^{-1}, respectively, for this species. Thus, the ν_3 value

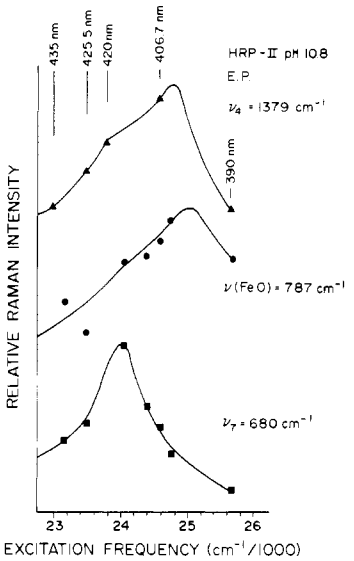

FIGURE 7: Excitation profiles of ν_7 = 680 cm^{-1}, ν(Fe=O) = 787 cm^{-1}, and ν_4 = 1379 cm^{-1}. The solid lines drawn for ν_7 and ν_4 represent the excitation profiles obtained by Bangcharochpaurpong et al. (1984) for the analogous modes in deoxymyoglobin.

of 1508 cm^{-1} for HRP-I (Figure 1b), unchanged from that of HRP-II (Figure 1c), and the absence of features in the 1590–1610-cm^{-1} range suggest that the species producing the spectrum in Figure 1b is not a porphyrin π-cation radical. Since the evidence for a porphyrin radical in HRP-I, particularly from ENDOR results (Roberts et al., 1981), is strong, we consider here possible explanations for the RR result.

Spin Delocalization. Using an approach similar to ours, but with CW excitation at 406.7 nm and high flow rates, Ogura and Kitagawa (1987) recently obtained a high-frequency RR spectrum of HRP-I, although with low signal-to-noise ratio. Their result is similar to our high-frequency spectrum (Oertling & Babcock, 1985; see also Figure 1b) and is also atypical of a MP$^{\bullet+}$. As these authors point out, extensive spin delocalization of the porphyrin radical onto the axial (oxoferryl)imidazole system might account for the absence of vibrations characteristic of the oxidized porphyrin in the RR spectrum of HRP-I. Delocalization of the porphyrin cation radical spin onto an axial pyridine ligand has been described for PyZnTPP$^{\bullet+}$ (Fujita et al., 1983). Perhaps more significant, the spin systems of the oxoferryl (S = 1) and porphyrin cation radical (S = $^1/_2$) may interact strongly in compound I structures (Schultz et al., 1984; Sontum & Case, 1985). While these factors may well influence vibrational frequency shifts between oxidized and neutral porphyrin complexes, this may not be sufficient to explain the essentially identical high-frequency RR spectra of HRP-II (pH 10.8) and HRP-I (pH 7) presented in Figures 4c–e and 5. ENDOR measurements clearly show that the unpaired electron in the radical site of HRP-I is hyperfine coupled to both ^{1}H and ^{14}N nuclei (Roberts et al., 1981). These could come from either the methine and b-carbon substituents and the pyrrole nitrogen of the porphyrin or from the α- and β-protons and imidazole nitrogen of the axial histidine. Thus, there is some ambiguity with the ENDOR measurements, and the delocalization model cannot be eliminated out of hand. Double-resonance experiments on HRP-I reconstituted with deuteriated protoheme, which would demonstrate that the radical site is indeed the porphyrin rather than the histidine, are mentioned by Roberts et al. (1981) but not presented.

Photochemistry. Both frozen and solution samples of HRP-I are known to undergo photoreaction when exposed to

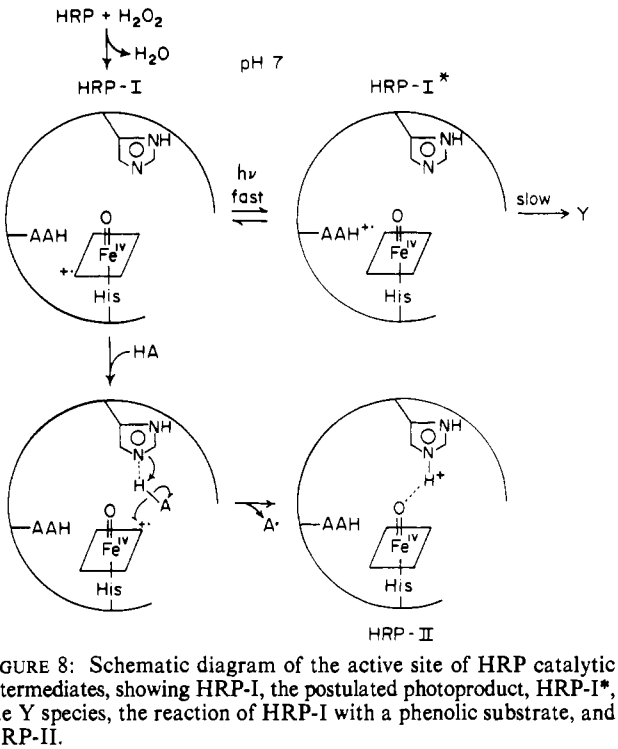

FIGURE 8: Schematic diagram of the active site of HRP catalytic intermediates, showing HRP-I, the postulated photoproduct, HRP-I*, the Y species, the reaction of HRP-I with a phenolic substrate, and HRP-II.

light in the Soret region (Stillman et al., 1975). The photoproduct, called Y, has an absorption spectrum similar to that of HRP-II (i.e., characteristic of ring-neutral heme) and gives an EPR signal of a free radical located on a protein residue (Chu et al., 1977). The quantum yield for this process is 0.003 (Nadezhdin & Dunford, 1979) and the rapid-mixing/pulsed Raman techniques used here were developed to avoid potential complications from Y formation. On the basis of the measured quantum yield, a maximum of ~10% conversion to Y might occur per laser pulse under our typical experimental conditions (1 mJ/laser pulse) if Y is formed in less than 10 ns. We estimate that at least ~20% conversion would be required for Y to begin to contribute significantly to the RR scattering. Furthermore, similar experiments with CW excitation at 406.7 nm at a wide range of flow rates carried out both in our lab (Figure 5b) and in Kitagawa's (Ogura & Kitagawa, 1987) as well as pulsed measurements at laser energies ranging from 0.5 to 2.0 mJ/pulse all produced similar results. These facts argue against not only artifacts due to photoconversion to Y but also artifacts due to possible scattering from excited states of HRP-I.

Although scattering from Y can be dismissed on the basis of measured quantum yield, the reversible formation of another ring-neutral photoproduct could explain the RR spectra we obtain for HRP-I. We denote this putative photoproduct as HRP-I* to acknowledge that it is distinct from Y and formally equivalent to HRP-I in oxidation state. In this model, the formation of HRP-I* is reversible and occurs in less than 10 ns with a quantum yield of ~0.01 or greater. Figure 8 depicts a possible relationship between HRP-I*, HRP-I, and Y. HRP-I* is formed by photoinduced electron transfer from a nearby amino acid to the porphyrin cation radical to produce a ring-neutral oxoferryl protoheme species and a protein-centered free radical. The resulting structure is formally equivalent to that which is thought to occur in cytochrome *c* peroxidase compound I (Hewson & Hager, 1979). The configuration of the oxoferryl protoheme in HRP-I* at neutral pH is postulated to be similar to that which occurs in HRP-II at high pH. This accounts for the similarity of the spectra

in Figures 4 and 5, as similar electronic distributions in the two species would produce similar excitation profiles. It also rationalizes our observation of similar frequencies and intensities ν(Fe=O) in HRP-I* and high pH HRP-II (Figure 3).

In Figure 8, HRP-I* is formed photochemically and can relax thermally to either HRP-I or Y. To account for our observation that HRP-I is the principal species we detect after the rapid-mixing Raman experiment, the branching ratio for the two thermal reactions must favor HRP-I heavily. Presumably, the initial amino acid oxidized in the thermal reaction transfers the hole back to the porphyrin with high yield to reform HRP-I; only in a small fraction of centers does the hole migrate to a more stable locus to form Y. The model proposed in Figure 8 can be tested by time-resolved optical experiments: The electronic properties of HRP-I and HRP-I* are expected to differ significantly, and the kinetic properties of Y and the proposed species should be distinct.

Both X-ray crystal structures (Spaulding et al., 1974; Gans et al., 1986) and our RR spectra of metalloporphyrin π-cation radicals (Oertling et al., 1987b) suggest that the isolated effects of macrocycle oxidation do not significantly change porphyrin core geometry. Thus, should our HRP-I RR result actually be due to an HRP-I* photoproduct, we speculate that the structural information contained in the time-resolved RR spectrum is relevant to the green $P^{\bullet+}$ form of HRP-I. Therefore, given either explanation (i.e., photochemistry or spin delocalization) for the similarity of the high-frequency RR scattering of HRP-I and HRP-II, the results presented in Figures 1 and 3 suggest that the core sizes of these two species are equal and that, at pH 7, the oxoferryl of HRP-I is not hydrogen-bonded.

Kinetics and Mechanism of HRP-I Reduction. A host of kinetic studies of the reaction of HRP-I with a variety of substrates suggests the involvement of a distal amino acid residue exhibiting a pK_a of 5.1, identified possibly as histidine 42 (His-42) (Dunford, 1982). For the substrates *p*-cresol and L-tyrosine, the reaction proceeds by a base-catalyzed mechanism. Figure 8 proposes a mechanism for the reaction of *p*-cresol with HRP-I at pH 7. The substrate is oriented by hydrogen bonding to distal His-42. This is consistent with studies that show that the acid form of *p*-cresol will bind to the cyanide complex of HRP at a distinct but nearby binding site at pH 7 (Critchlow & Dunford, 1972). As an electron is transferred from the substrate to the porphyrin cation radical, a proton is transferred along the hydrogen bond to His-42. This homolytic cleavage of the H–A bond (or H–O bond of *p*-cresol) results in the formation of the free radical of the substrate (Shiga & Imizuni, 1975) along with HRP-II. The oxoferryl of HRP-II is hydrogen bonded to the protonated His-42 residue (Sitter et al., 1985b; Hashimoto et al., 1986). The reaction of HRP-II with the substrate is influenced by an acid group with pK_a of 8.6 (Dunford, 1982). Thus, the participating acid group is most likely His-42 in both cases as was speculated earlier (Job & Dunford, 1976). The pK_a is shifted by the positive charge of the porphyrin cation in HRP-I. This mechanism is consistent with Hammett and Okamoto-Brown plots constructed from rate constants for the reduction of HRP-I by a series of substituted phenols. These were taken to suggest a mechanism wherein the neutral substrate donates an electron to HRP-I and simultaneously loses a proton (Job & Dunford, 1976).

Added in Proof

In another peroxidase enzyme, prostaglandin H synthase, recent work (Karthein et al., 1988; Dietz et al., 1988) has suggested the occurrence of a distinct intermediate formed by intramolecular electron transfer from a tyrosine residue to the porphyrin π-cation radical of compound I resulting in a two-electron-oxidized state consisting of an oxoferryl ring-neutral heme and a tyrosine cation radical. This state precedes the traditional compound II state in the catalytic cycle of this enzyme. Thus, the work presented here and that mentioned above, together with the long-standing controversy as to the radical location in cytochrome *c* peroxidase compound I [cf. Edwards et al. (1987)], suggest that a mobility of the second oxidation equivalent in the peroxidase active site may be a general feature of these enzymes.

Acknowledgments

We thank Drs. T. Kitagawa and J. E. Penner-Hahn for manuscripts prior to publication. T.O. thanks A. Salehi for technical assistance and Dr. H. B. Dunford for discussion.

References

Abe, M., Kitagawa, T., & Kyogoku, Y. (1978) *J. Chem. Phys. 69*, 4526–4534.

Asada, K., & Badger, M. R. (1984) *Plant Cell Physiol. 25*, 1169–1179.

Bangcharoenpaurpong, K. T., Schomacher, K. T., & Champion, P. M. (1984) *J. Am. Chem. Soc. 106*, 5688–5698.

Callahan, P. M., & Babcock, G. T. (1981) *Biochemistry 20*, 952–958.

Chance, B. (1949) *Arch. Biochem. 22*, 224–252.

Chappacher, M. Chottard, G., & Weiss, R. (1986) *J. Chem. Soc., Chem. Commun. 2*, 93–94.

Choi, S., Spiro, T. G., Langry, K. C., Smith, K. M., Budd, D. L., & LaMar, G. N. (1982) *J. Am. Chem. Soc. 104*, 4345–4351.

Chu, M., Dunford, H. B., & Job, D. (1977) *Biochem. Biophys. Res. Commun. 74*, 159–164.

Critchlow, J. E., & Dunford, H. B. (1972) *J. Biol. Chem. 247*, 3714–3725.

Dietz, R., Nastainczyk, W., & Rut, H. H. (1988) *Eur. J. Biochem. 171*, 321–328.

Dolphin, D., Forman, A., Borg, D. C., Fajer, J., & Felton, R. H. (1971) *Proc. Natl. Acad. Sci. U.S.A. 68*, 614–618.

Dunford, H. B. (1982) *Adv. Inorg. Biochem. 4*, 41–68.

Dunford, H. B., & Cotton, M. L. (1975) *J. Biol. Chem. 250*, 2920–2932.

Dunford, H. B., & Stillman, J. S. (1976) *Coord. Chem. Rev. 19*, 187–251.

Edwards, S. L., Xuong, N. L., Hamlin, R. C., & Kraut, J. (1987) *Biochemistry 26*, 1503–1511.

Felton, R. H., Romans, A. Y., Yu, N.-T., & Schonbaum, G. R. (1976) *Biochim. Biophys. Acta 434*, 82–89.

Frew, J. E., & Jones, P. (1984) *Adv. Inorg. Bioinorg. Mech. 3*, 175–213.

Fujita, I., Hanson, L. K., Walter, F. A., & Fajer, J. (1983) *J. Am. Chem. Soc. 105*, 3296–3300.

Gans, P., Buisson, G., Dûee, E., Marchon, J.-C., Erler, B. S., Scholtz, W. F., & Reed, C. A. (1986) *J. Am. Chem. Soc. 108*, 1223–1234.

Hashimoto, S., Tatsuno, Y., & Kitagawa, T. (1984) *Proc. Jpn. Acad., Ser. B 60*, 345–348.

Hashimoto, S., Tatsuno, Y., & Kitagawa, T. (1986) *Proc. Natl. Acad. Sci. U.S.A. 83*, 2417–2421.

Hashimoto, S., Tatsuno, Y., & Kitagawa, T. (1987) *J. Am. Chem. Soc. 109*, 8096–8097.

Hewson, W. D., & Hager, L. P. (1979) *Porphyrins 7*, 295–332.

Job, D., & Dunford, H. B. (1976) *Eur. J. Biochem. 66*, 607–614.

Karthein, R., Dietz, R., Nastainczyk, W., & Rut, H. H. (1988) *Eur. J. Biochem. 171*, 313-320.
Kean, R. T., Oertling, W. A., & Babcock, G. T. (1987) *J. Am. Chem. Soc. 109*, 2185-2187.
Nadezhdin, A. D., & Dunford, H. B. (1979) *Photochem. Photobiol. 29*, 899-903.
Naqui, A., & Chance, B. (1986) *Annu. Rev. Biochem. 55*, 137-166.
Oertling, W. A., & Babcock, G. T. (1985) *J. Am. Chem. Soc. 107*, 6406-6407.
Oertling, W. A., Salehi, A., Chang, C. K., & Babcock, G. T. (1987a) *J. Phys. Chem. 91*, 3114-3116.
Oertling, W. A., Salehi, A., Chung, Y., Leroi, G. E., Chang, C. K., & Babcock, G. T. (1987b) *J. Phys. Chem. 91*, 5887-5898.
Oertling, W. A., Salehi, A., Chang, C. K., & Babcock, G. T. (1988) *J. Phys. Chem.* (submitted for publication).
Ogura, T., & Kitagawa, T. (1987) *J. Am. Chem. Soc. 109*, 2177-2179.
Penner-Hahn, J. E., Smith-Eble, K., McMurry, T. J., Groves, J. T., Dawson, J. H., & Hodgson, K. O. (1986) *J. Am. Chem. Soc. 108*, 7819-7825.
Proniewicz, L. M., Bajdor, K., & Nakamoto, K. (1986) *J. Phys. Chem. 90*, 1760-1766.
Rakhit, G., & Spiro, T. G. (1976) *Biochem. Biophys. Res. Commun. 71*, 803-808.
Roberts, J. E., Hoffman, B. M., Rutter, R., & Hager, L. P. (1981) *J. Biol. Chem. 256*, 2118-2121.
Salehi, A., Oertling, W. A., Babcock, G. T., & Chang, C. K. (1986) *J. Am. Chem. Soc. 108*, 5630-5631.
Salehi, A., Oertling, W. A., Babcock, G. T., & Chang, C. K. (1987) *Inorg. Chem. 26*, 4296-4298.
Schonbaum, G. R., & Lo, S. (1972) *J. Biol. Chem. 247*, 3353-3360.
Schultz, C. E., Rutter, R., Sage, J. T., Debrunner, P. G., & Hager, L. P. (1984) *Biochemistry 23*, 4743-4754.
Shiga, T., & Imaizumi, K. (1975) *Arch. Biochem. Biophys. 167*, 469-479.
Sitter, A. J., Reczek, C. M., & Terner, J. (1985a) *Biochim. Biophys. Acta 828*, 229-235.
Sitter, A. J., Reczek, C. M., & Terner, J. (1985b) *J. Biol. Chem. 260*, 7515-7522.
Sontum, S. F., & Case, D. A. (1985) *J. Am. Chem. Soc. 107*, 4013-4015.
Spaulding, L. D., Eller, P. G., Bertrand, J. A., & Felton, R. H. (1974) *J. Am. Chem. Soc. 96*, 982-987.
Stillman, J. S., Stillman, M. J., & Dunford, H. B. (1975) *Biochemistry 14*, 3183-3188.
Terner, J., & Reed, D. E. (1984) *Biochim. Biophys. Acta 789*, 80-86.
Terner, J., Sitter, A. J., & Reczek, C. M. (1985) *Biochim. Biophys. Acta 828*, 73-70.
Van Wart, H. E., & Zimmer, J. (1985) *J. Am. Chem. Soc. 107*, 3379-3381.
Worthington Enzyme Manual (1972) p 41, Worthington Biochemical Corp., Freehold, NJ.

A Fourier-Transform Infrared Spectroscopic Study of the Phosphoserine Residues in Hen Egg Phosvitin and Ovalbumin†

Jose M. Sanchez-Ruiz‡ and Marino Martinez-Carrion*
School of Basic Life Sciences, Division of Molecular Biology and Biochemistry, University of Missouri—Kansas City, Kansas City, Missouri 64110

Received July 10, 1987; Revised Manuscript Received January 7, 1988

ABSTRACT: A Fourier-transform infrared spectroscopic study of hen egg phosvitin and ovalbumin has been carried out. Bands arising from monoanionic and dianionic phosphate monoester [Shimanouchi, T., Tsuboi, M., & Kyogoku, Y. (1964) *Adv. Chem. Phys. 8*, 435-498] can be identified easily in the 1300-930 cm^{-1} region in spectra of solutions of *O*-phosphoserine and phosvitin, a highly phosphorylated protein. On the other hand, spectra of ovalbumin show a relatively strong absorption above 1000 cm^{-1} arising from the protein moiety. Below 1000 cm^{-1}, a single band at 979 cm^{-1} is observed; this band is not present in spectra of dephosphorylated ovalbumin, and therefore, it has been assigned to the symmetric stretching of the phosphorylated Ser-68 and Ser-344 in the dianionic ionization state. In addition, bands arising from symmetric and antisymmetric stretchings of the monoanionic ionization state, and from the antisymmetric stretching of the dianionic state, can be detected above 1000 cm^{-1} in difference spectra of ovalbumin minus dephosphorylated ovalbumin. The effect of pH on the infrared spectra of *O*-phosphoserine, phosvitin, and ovalbumin is consistent with the phosphoserine residues undergoing ionization with p*K* values about 6. This study demonstrates that Fourier-transform infrared spectroscopy can be a useful technique to assess the ionization state of phosphoserine residues in proteins in solution.

We have recently shown that Fourier-transform infrared (FTIR)[1] spectroscopy can be a valuable technique to determine the ionization state of protein-bound phosphoryl groups for coenzyme-dependent enzymes (Sanchez-Ruiz & Martinez-Carrion, 1986).

Information regarding ionization states of bound phosphoryl groups may, in many cases, not be obvious on the basis of ^{31}P NMR chemical shift studies, as the phosphorus chemical shift is sensitive to factors other than the charge on the phosphoryl group, such as the O-P-O bond angle [Gorenstein, 1975; for

† This research was supported by U.S. Public Health Service Grants GM-38184 and HL-38412.

‡ Recipient of a Fulbright-Spanish Ministry of Education and Science Scholarship for the period September 1984-June 1986. Present address: Department of Physical Chemistry, University of Granada Granada, Spain.

[1] Abbreviation: FTIR, Fourier-transform infrared.

0006-2960/88/0427-3338$01.50/0